ACADÉMIE DE LA RÉPUBLIQUE SOCIALISTE DE ROUMANIE

REVUE ROUMAINE DE PHYSIQUE

TIRAGE À PART

TOME 34
1989
N° 3

EDITURA ACADEMIEI REPUBLICII SOCIALISTE ROMÂNIA

NUMERICAL TRANSPORT STUDIES BASED ON TOKAMAK EXPERIMENTAL DATA*

F. SPINEANU **, M. VLAD **, J. BADALEC ***, J. STÖCKEL ***, F. ŽÁČEK ***

**Institute of Physics and Technology of Radiation Devices, Bucharest, Măgurele, P. O. Box MG-7, Romania

*** Institute of Plasma Physics, Czechoslovak Academy of Sciences, Pod vodárenskou věží 4, 182 11 Prague 8, Czechoslovakia

A model of the dynamics of the plasma in the tokamak CASTOR is proposed. It is shown that a small amount of experimental data may provide rich qualitative and even quantitative information when they are used with a system of related models and computer codes. Actually, the method consists in breaking the self-consistent system of transport equations (1)—(4) in a chain of interconnected equations which are easier to be numerically solved separately. A large number of iterative trials can be performed in order to reproduce the experimental data with the constraint that self-consistency is approximately fulfilled. Besides, an estimate of the transport coefficients results. Using this information, the full model and large computer codes determine a credible picture of the discharge dynamics and a good estimation of plasma parameters.

1. INTRODUCTION

In order to understand the evolution of the plasma in a tokamak discharge, besides the experimental work, it is necessary to perform theoretical and computational studies devoted to the identification of the transport model. These studies often provide new information which is only implicit in the rough experimental results. In fact, each tokamak device imposes particular features on plasma behaviour which are not easily inferred from the general theoretical frame. This paper is an attempt to build a system of computer codes, having different complexity levels, and a method of using them in connection with a small amount of experimental data as an efficient tool in identifying the transport model and in estimating some plasma parameters which are not experimentally determined.

The exemplification of this method is performed on the CASTOR tokamak (a small device $R = 0.40$ m, $a = 0.075$ m, $B_T = 1.3$ T) working at the Institute of Plasma Physics in Prague. The specific feature of this tokamak is the evolution of the space-averaged electron density which has a fast growth, followed by an exponential decay instead of the quasistationary regime observed in other devices (Fig. 1.b). These weak particle confinement characteristics are compensated by feeding the discharge using the gas puffing procedure. This study being focused on

* Received December 4, 1987

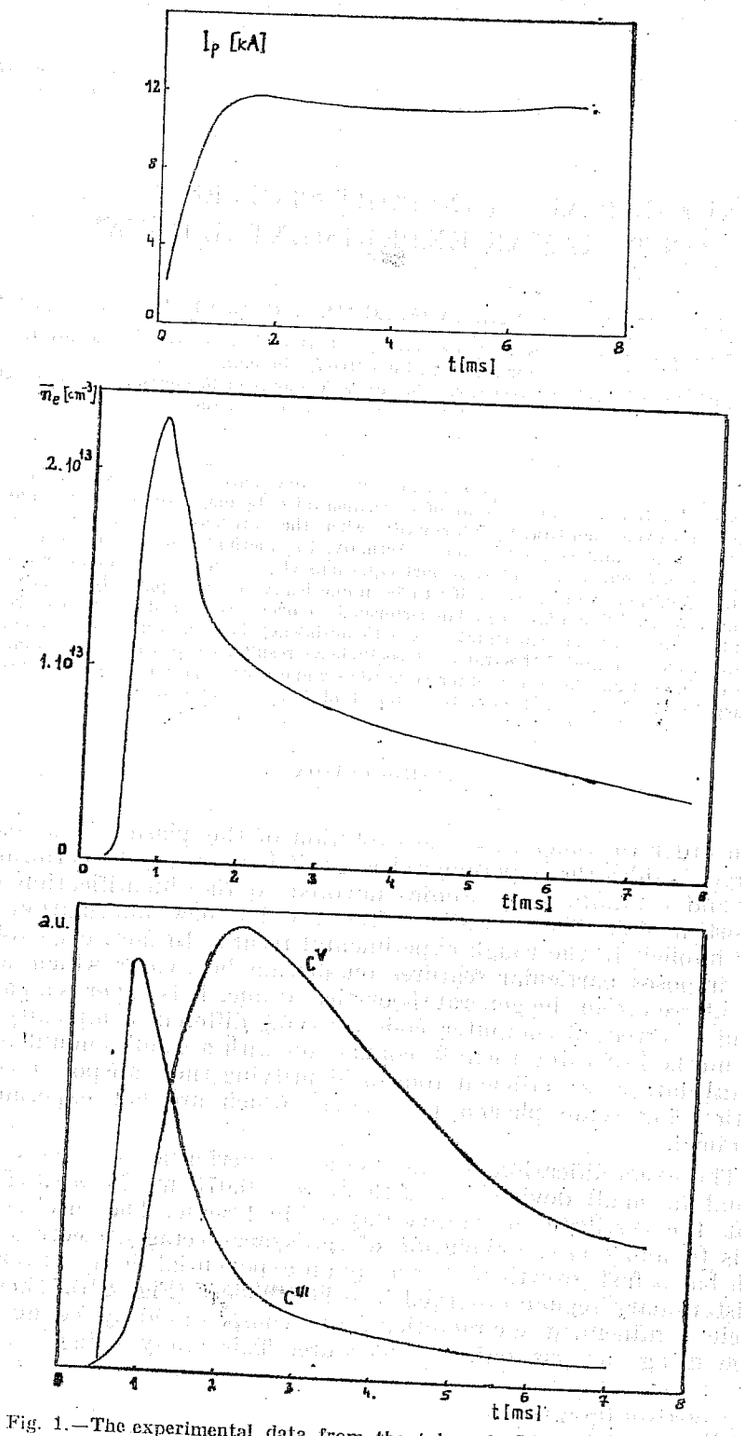

Fig. 1.—The experimental data from the tokamak CASTOR; a) the total plasma current as a function of time; b) the time evolution of the average electron density; c) the time dependence of the intensities of line radiation from C^{III} ($\lambda = 2296$ Å) and C^{V} ($\lambda = 2270$ Å), integrated on plasma diameter.

understanding the conditions of the anomalous particle losses, the gas puffing is not taken into account. Besides the temporal evolution of the average electron density and of the total plasma current (Fig. 1. a, b), the intensities of two line radiation from the carbon impurity atoms, integrated on plasma diameter, (Fig. 1. c) are the only experimental data used in connection with numerical computations.

The numerical study consists of two stages. The first stage contains a very large number of runs of some interconnected, small codes based on simplified physical models which determine the approximate plasma parameters as well as the transport model consistent with experimental data. In the second stage, using large computer codes based on extended models, the predictions of the first stage are verified and corrected. Introducing the estimated transport model in the complete transport code, the credible evolution of the plasma parameters is determined.

A brief description of the models and of the codes used in this study is presented in §2. §3 contains the main results while the conclusions are summarized in §4.

2. MODELS AND CODES

The theoretical study of the tokamak plasma evolution relies on the transport processes of particles and energy. The main plasma and field parameters are the solution of the following set of partial differential equations representing the energy balance for electrons (1) and ions (2), the diffusion of particles (3) and Maxwell's equations (4,5) in 1-dimensional geometry corresponding to axial symmetry:

$$\frac{3}{2}\frac{\partial}{\partial t}(n_e T_e) = -\frac{1}{r}\frac{\partial}{\partial r}\left(r\left(q_e + \frac{3}{2}n_e V T_e\right)\right) - 3\frac{m_e}{m_p}\frac{T_e - T_i}{\tau_e}[Z]n_e + EJ - Q_{rad} - f(t)n_e n_0 \langle \sigma_{ion} v(T_e)\rangle \quad (1)$$

$$\frac{3}{2}\frac{\partial}{\partial t}(n_e T_i) = -\frac{1}{r}\frac{\partial}{\partial r}\left(r\left(q_i + \frac{3}{2}n_e V T_i\right)\right) + 3\frac{m_e}{m_p}\frac{T_e - T_i}{\tau_e}[Z]n_e - n_p n_0 R_{cx}\frac{3}{2}(T_i - T_0) - n_e n_0 \langle \sigma_{ion} v(T_e)\rangle \frac{3}{2}T_0 \quad (2)$$

$$\frac{\partial n_e}{\partial t} + \frac{1}{r}\frac{\partial}{\partial r}(r\Phi) = n_e n_0 \langle \sigma_{ion} v(T_e)\rangle + S_{imp} \quad (3)$$

$$J = \frac{1}{r}\frac{\partial}{\partial r}(rB_\theta) \quad (4)$$

$$\frac{\partial B_\theta}{\partial t} = \frac{\partial E}{\partial r}; \quad E = \eta J \quad (5)$$

Here, the usual notations are utilized. m_e, n_e, T_e=electron mass, density and temperature; m_p, n_p, T_i = ion mass, density and temperature; J = plasma current density; B_0 = poloidal magnetic field; E = toroidal electric field; τ_e = the inverse of the electron-ion collision frequency ν_e; V = the radial diffusion velocity of particles; Φ = the particle diffusion flux, $\Phi = n_e V$. The thermal conductibility fluxes have the form:

$$q_a = - n_a \chi_a \frac{\partial T_a}{\partial r}; \quad a = e, i \tag{6}$$

χ_a being the corresponding conductibility coefficient. The expression of the electron diffusion flux in equation (3) contains both the neoclassical part and the anomalous inward pinch determined by the banana orbits [1]:

$$\Phi = - D \frac{\partial n_e}{\partial r} + n_e \tilde{\Gamma}; \qquad \tilde{\Gamma} = \alpha \frac{E}{B_0} \left(\frac{r}{R} \right)^2 \tag{7}$$

The plasma in the CASTOR tokamak being far from the neoclassical banana regime, low values were attributed to the parameter α which is a measure of the importance of the phenomenon ($\alpha \in [0,10]$).

In the initial stage, the radiation from the neutral atoms of hydrogen and the complexity of the ionization processes determine large losses of energy (greater than the fundamental energy) for each newly created electron-proton pair [2]. A time dependent coefficient $f(t)$ is introduced in the power lost by electrons through ionization in equation (1) in order to account for this process:

$$f(t) = 13.6 \left(1 + \frac{200}{13.6} \exp\left(-t/\tau_1\right) \right) \tag{8}$$

The neutral atom density $n_0(r, t)$ is simply described as an exponential decay in time of a radial profile also determined by an exponential radial dependence:

$$n_0(r, t) = N_0 \exp\left(-t/\tau_2\right) \exp\left(-(a - r)/r_0\right) \tag{9}$$

$\langle \sigma_{ion} v \rangle$ and R_{cx} are the ionization and charge exchange rates used in the context of the neutral gas influence on the energy balance. The values of the parameters τ_1, τ_2, r_0, N_0 appropriate for the description of the CASTOR discharge were found to range respectively in the intervals: (0.20 — 0.30) ms, (0.4—0.6) ms, (0.2—0.3)$\times a$ and (0.6 10^{13} —1.10^{13})cm^{-3}.

The density of radiated power Q_{rad} and the effective charge $[Z]$ are determined assuming corona equilibrium for the impurity stages of ionization. A more accurate description of the impurity evolution was also used in connection with plasma transport model (1)—(5). It consists in solving a diffusion equation for the total impurity density and in distributing this density on the ionization stages according to the corona equilibrium. In the frame of the neoclassical transport corrresponding to CASTOR tokamak, this model leads to unphysical results (strong accumulations in the central region and singular behaviour of the effective charge at plasma border). This suggested the necessity of a more detailed

study of impurity dynamics which, due to its complexity, was performed separately from the plasma transport code.

In the electron temperature equation (1), the boundary condition $T_e(r = a)$ is time dependent, the value being obtained by solving an approximate energy balance equation at this point. The other parameter boundary conditions are constant values.

The specific transport model is contained in the expression of the coefficients D, χ_e, χ_i appearing in the fluxes of particles and heat. The basic theoretical model indicated for the CASTOR tokamak conditions is the high collisional limit of the neoclassical regime (Pfirsch-Schluter). The corresponding expressions for the coefficients are:

$$\chi_e = \nu_e \rho^2 (1 + 0.6\, q^2)$$

$$\chi_i = 1.41\ \nu_i \rho_{i0}^2 (r/R)^{1/2} \tag{10}$$

$$D \cong \chi_e/5$$

Here ρ is the electron Larmor radius, q is the safety factor, ν_i is the ion collision frequency and ρ_{i0} is the ion Larmor radius corresponding to the poloidal magnetic field.

The set of equations (1) — (5) was numerically solved by means of the computer code described in [3].

The selection of the parameters of the physical model which could reproduce some particular experimental data implies usually a large number of computer runs. The code based on the selfconsistent system of equations (1)—(5) is a difficult tool in this attempt. Besides, it did not clearly reveal the relative influences of different characteristics of the plasma (e.g. densities and temperatures). The use of simplified models in a first stage of the numerical study is recommended. A separated study for the impurity dynamics and for the electron density evolution was performed in connection with the set of experimental data from CASTOR tokamak (line intensities from carbon ions and average electron density).

The space-time dependences of the densities of impurity ion species in each stage of ionization ($n_k(r, t)$, $(k - 1)$ e = electric charge) are determined from a system of diffusion type equations representing the particle number conservation:

$$\frac{\partial n_k}{\partial t} + \frac{1}{r} \frac{\partial}{\partial r} (r \Phi_k) + n_{k-1}(-n_e \alpha_k) + n_k n_e (\beta_k + \alpha_{k+1}) +$$

$$+ n_{k+1}(-n_e \beta_{k+1}) = S_k \qquad k = 1, \ldots, Z + 1 \tag{11}$$

Here, α_k is the ionization coefficient to the kth state, β_k is the recombination coefficient from the kth state and S_k is the source of impurity ions in the kth state of ionization.

The diffusion flux of the impurity ions Φ_k contains both the neoclassical term and an anomalous contribution. It has the general form:

$$\Phi_k = a_k \frac{\partial n_k}{\partial r} + b_k n_k \tag{12}$$

where a_k and b_k are functions of r and t and of the plasma parameters. The expressions used by the TFR group were adopted.

The numerical codes used to solve this system of equations are described in [4], [5].

Neglecting the diffusion flux and supposing that the equilibrium condition is attained $\left(\frac{\partial}{\partial t} = 0\right)$, the corona model is obtained. The long series of runs aimed at the computed reproduction of C^{III} and C^{V} experimental line intensity evolutions were performed in these simplified conditions. The input parameters were the total densities of C and O and, most important, the electron temperature $T_e(r, t)$. The influence of the diffusion was studied only after such a rough estimation of the space time dependence of the electron temperature.

The electron density equation (3) was solved separately from the whole system (1) — (5) in order to study the influence of the following parameters: electron temperature $T_e(r, t)$, diffusion D and coefficient α of the inward pinch. [6] The source of electrons from the ionization of the neutral hydrogen gas was computed using an interpolation formula given in [7]. The source from impurity ionization was obtained by the impurity code with the same $T_e(r, t)$.

These two codes used in tandem provide a delimitation of the electron temperature profile and time dependence compatible with experimental data. An additional verification of this result is obtained by solving a simplified (space integrated) energy balance equation which gives the evolution of the average electron temperature:

$$\frac{\mathrm{d}}{\mathrm{d}t}\left(\frac{3}{2}\bar{n}\bar{T}_e\right) = 0.09\,\bar{T}_e^{-3/2} Z_{\mathrm{eff}} (I_p(t)/\pi/a^2)^2 -$$

$$- f(t)\bar{n}\, n_0 \exp(-t/\tau_1)\langle\sigma_{\mathrm{ion}} v\rangle - P_{\mathrm{rad}} - \frac{3}{2}\bar{n}\bar{T}_e/\tau_0 \tag{13}$$

where Z_{eff} and P_{rad} are provided by the impurity code, τ_0 is the energy confinement time ($\tau_0 \simeq a^2/\chi_e$) and $I_p(t)$ is the total plasma current.

These three simplified models constitute an interconnected chain of codes which was used in connection with experimental data according to the scheme presented in Fig. 2.

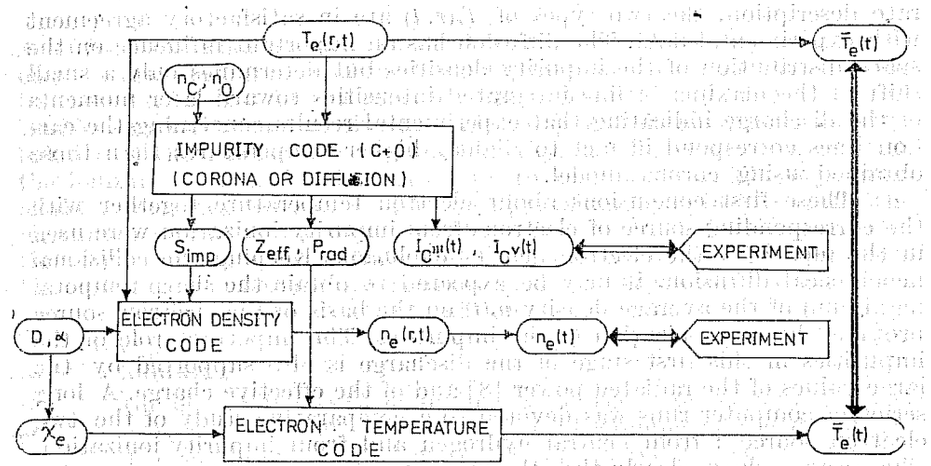

Fig. 2. — The interconnection relations between the simplified models and the computer codes.

3. RESULTS

According to the previous section, the first step in obtaining information about the discharge is to determine the qualitative features of the space-time dependence of the electron temperature. It consists in computing the intensities of line radiation for C^{III} and C^{V} given by the corona model for various functions $T_e(r, t)$. The experimental data suggest that the electron temperature rapidly exceeds the value of 4—5eV (which gives the maximum of population for C^{III}) and increases with a slow rate reaching the maximum of population of C^{V} (at about 30 eV) only after 2 mseconds. Taking into account the fact that the experimental data are line integrated, the necessity of a careful examination of the spatial distribution of electron temperature arises. A long series of computer runs lead to the conclusion that the computed line intensities are very sensitive to the function $T_e(r, t)$ and that only two types (physically allowed) of space-time dependences provide results close to the experimental ones:

- a broad (parabolic) radial profile rising slowly in time, reaching about 10 eV at 1 ms and 30 eV at 2 ms;
- a radial profile with a strong nonuniformity, having a narrow maximum in the centre and a large marginal zone of low, quasi-uniform temperature. The central maximum rises fast in time (to about 250 eV in 2 ms) and saturates while the marginal zone, extending approximately on half of the plasma radius, has the temporal dynamics of the previous case.

In both cases, the necessity of obtaining a rapid fall of C^{III} line intensity requires to increase the boundary value of the temperature from 1eV to 5—7 eV in the first millisecond.

A series of computer runs with the full impurity evolution model (including neoclassical diffusion) confirms that, even in this more accu-

rate description, the two types of $T_e(r, t)$ are in satisfactory agreement with experimental data. The diffusion has an important influence on the space distribution of the impurity densities but determines only a small shift of the maxima of line integrated intensities toward later moments of the discharge indicating that experimental results concerning the carbon lines correspond in fact to slightly higher temperatures than those obtained using corona model.

These first conclusions about electron temperature together with the corresponding source of electrons from impurity ionization were used in the model for the electron density evolution. Keeping the collisional neoclassical diffusion, it may be expected to obtain the sharp temporal maximum of the average density $n_e(t)$ on the basis of the electron source provided by the ionization of the impurities. The important role of the impurities in this first stage of the discharge is also supported by the large values of the radiated power [8] and of the effective charge. A long series of computer runs was devoted to a comparative study of the two electron sources : from neutral hydrogen and from impurity ionization. The results show clearly that the impurity source cannot overcome the neutral hydrogen source of electrons. These sources determine that fast increase of the electron density but, even when they are almost vanishing and the density dynamics remains to be dominated by diffusion losses, it is not possible to obtain the experimental decay of n_e. This indicates the existence of an anomalous diffusion mechanism in this stage of the discharge.

The aim of the next series of computer runs was the estimation of the diffusion coefficient which is in agreement with the electron losses observed in experiments. A result of this investigation consists in eliminating the broad radial profile of the electron temperature. It would imply an important ionization at later time moments ($t > 1$ ms) which partly compensates the anomalous diffusion losses and the average density cannot have the observed rate of decrease. It seems that only the model of warm central plasma channel is able, in the frame of these simplified calculations, to reproduce the experimental data concerning both the carbon line intensities and the average density evolution.

Because the Pfirsch-Schluter diffusion coefficient is generally valid for low temperature tokamak plasma, the anomalous diffusion coefficient was taken of the form :

$$D = D_{PS}(1 + c(1 - \exp(-t^2/\alpha))) \qquad (14)$$

where c and α are constants to be determined from the comparison of the computed results with the experimental ones. In this expression, the diffusion coefficient is of the Pfirsch-Schluter type at the beginning of the discharge ($t \to 0$) when the collision frequency is very large and there is no reason for any instability to develop and, gradually departs from this value with a time depending factor. The values of the parameters c and α which ensure the experimental rate of decay of the electron density were about 1000 and respectively 8.

In order to have a supplementary control on the selfconsistency of these separate evaluations, the 0-dimensional energy balance equation for electrons (13) was solved and the average temperature determined.

A satisfactory concordance between this result and the space average on the warm central zone of the temperature which was determined to be the best input data in the previous calculations, was obtained (Fig. 4). Besides, an estimation of the dynamics of powers implied in the energy balance of the plasma was determined (Fig. 5). The power lost through the ionization channel is important up to 1 millisecond. The maximum of the power radiated from impurities approximately coincides with the maximum of the average electron density ($t = 1$ ms). In these simulations, made without gas puffing, the radiation channel is no more important after 2 ms when the temperature evolution begins to be determined only by ohmic heating and thermal conduction.

The principal conclusions of this chain of interconnected models are the following :

- the plasma is heated nonuniformly on the cross section, a warm central region developing from the beginning of the discharge. The low temperature marginal zone, having a slow evolution in time, determines the main contribution to the line radiation from impurities ;
- an anomalous transport mechanism develops leading to high particle losses.

More specifically these studies allow an evaluation of the diffusion coefficient. Besides, they lead to an approximate picture of the main parameter evolution and of their relative influences which are not evident in the full model.

These conclusions are in agreement with the results of the full, selfconsistent system of transport equations. The simulations performed starting from the parabolic initial radial profile for electron temperature show a fast heating of the central zone leading to the formation of a central warm channel in the plasma. With the neoclassical collisional transport coefficients, this central channel develops in time to an unphysical very narrow, high peak of both temperature and current density showing the onset of a thermal instability in the numerical simulation. Furthermore, no tendency of electron density decay is obtained.

This unphysical explosive growth of the central temperature could be explained by not including in the simulation one of the following phenomena :

- the existence of a run-away component in the electric current ;
- the onset of some plasma instabilities.

Both possibilities were studied by means of the large transport code.

The radial distribution of the run-away electron density was supposed to exponentially decrease toward plasma edge and to have central values up to 20 % of the total current density. This component does not contribute to the ohmic heating of electrons and it was extracted from the current density contained in the electron temperature equation (1) and in the Ohm's equation. Maxwell's equations were not modified. The results of these simulations indicate a small decay of the temporal rate of growth of the central temperature but the explosive evolution of the central channel cannot be hindered.

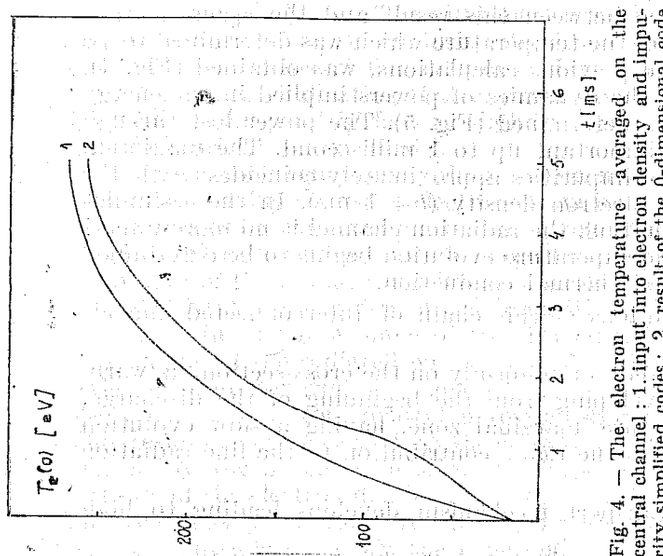

Fig. 4. — The electron temperature averaged on the central channel : 1. input into electron density and impurity simplified codes ; 2. result of the 0-dimensional code for temperature time evolution.

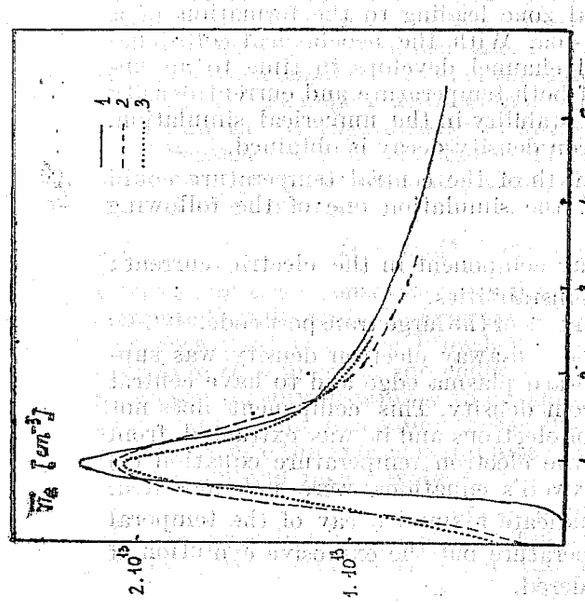

Fig. 3. — The time evolution of the average electron density : 1. experimental ; 2. result of simplified model ; 3. result of the full transport code.

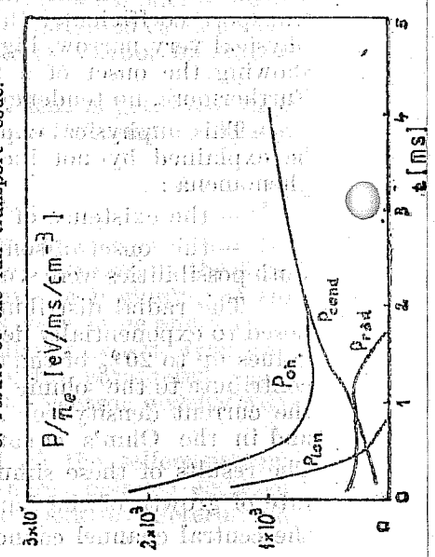

Fig. 5. — The power balance as determined from the 0-dimensional code for electron temperature evolution.

At this low temperature, high collisionality regime, the possible instabilities leading to anomalous transport are of dissipative electrostatic type [9]. In fact, detailed analysis indicates that, in the presence of a magnetic shear, the dissipative drift wave is stable [10]. However, the instability can appear if some physical factor acts to localise the mode energy, lowering the shear damping. It has been demonstrated [11] that a high electron temperature gradient provides such a mechanism and destabilises the drift wave, altering the balance between the time dependent thermal force and the local resistive absorption of energy.

The previous studies indicate the existence of such large electron temperature gradient associated with the presence of the warm central channel in plasma. In the case of low shear of the confining magnetic field, the unstable mode has the growth rate :

$$\gamma \cong (k_\perp \rho_s c_s / L_T)^2 / \nu_e \tag{15}$$

where $k_\perp^{-1}$ is the wavelength perpendicular to the confining magnetic field, $L_T = \left(\frac{\partial \ln T_e}{\partial r} \right)^{-1}$ is the characteristic length for temperature variation, $c_s = \sqrt{T_e/m_i}$ is the ion sound speed and $\rho_s = (m_i c_s)/(eB)$ is the ion Larmor radius based on T_e. ν_e is the electron-ion collision frequency. The thermal conductibility can be estimated as $\chi_e = \text{const.}\, D$ using Kadomtsev's formula :

$$D \cong \gamma / k_\perp^2 \tag{16}$$

In the specific conditions of the tendency of explosive growth of central temperature, χ_e is characterized by a small value in the centre of the plasma ($\nabla T_e = 0$), has a maximum at the limit of the central channel ($r = a/2$) and decays to the plasma border. The results of the simulation clearly show that the presence of this instability and of the associated transport avoid the explosive evolution of the central region transferring an amount of energy to the cold plasma of the marginal region. However, the radial dependence of the electron temperature is still characterized by the existence of a warm central channel as seen from the evolution of the peaking ratio $T_e(O)/\bar{T}_e$ presented in Fig. 8. This feature of CASTOR discharge, also deduced in [8], is determined mainly by the dynamics of the current density. The time of current penetration ($\tau_{skin} = 2$ ms) is greater than the total plasma current rise time (1 ms) which implies that the current density expands slowly from the central core to the plasma border. This explains the development of a central warm channel in the plasma while the cooling by impurity radiation is only an additional cause in the initial stage ($t > 1$ ms).

The diffusivity (15), (16), having small values at the plasma border, cannot determine the experimental decay of the average electron density. The anomalous diffusion coefficient estimated by the previous simplified calculations (14) must be added. In the simulations performed

with the full transport code, this was introduced with a dependence on the plasma parameters of the Pfirsch-Schluter type (characterized by large values at the border and small values in the centre) as in (14). However, it was found that the time dependent factor must be modified in order to get the shape of the experimental average electron density evolution (Fig. 3). The resulting χ_e is shown in Fig. 7.

This coefficient may be determined by the electrostatic drift wave turbulence. Rough estimates of the particle diffusion based on the "mixing length" assumption : $D = k_\perp \gamma L_n^2 (\tilde{n}_e/n_e)^2$ with $k_\perp \rho_s \simeq 0.3$, $\gamma = 0.1\ \omega_*$ (where $\omega_* = (k_\perp T_e)/(eBL_n)$ is the drift wave frequency) together with the values found for $D (D = \chi_e/1.5$, χ_e given in Fig. 7) would imply a level of density fluctuations $\tilde{n}_e/n_e \approx 80 - 100\%$ in the outer region of the plasma and $\tilde{n}_e/n_e \approx 10-20\%$ in the central zone.

The set of results presented in Figs 8—12 is obtained from a discharge simulation which begins with the following conditions : $n_e = 3.2 \cdot 10^{12}$ cm^{-3}, uniform on the radius ; $T_e(0) = 5$eV ; $T_i(0) = 1$eV ; $I_p = 1$kA, reaching 12kA in 1ms. The neutral atom density and the car-

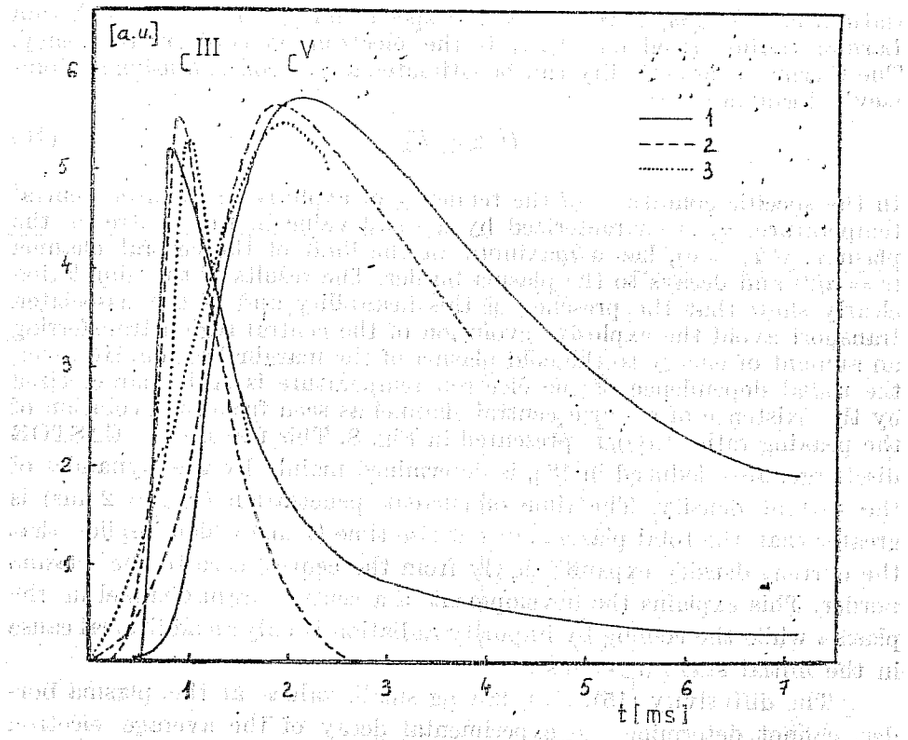

Fig. 6. — The intensities of line radiation from C^{III} ($\lambda = 2296$ Å) and C^{V} ($\lambda = 2270$ Å) : 1. experimental ; 2. result of the simplified model ; 3. result of the full transport code.

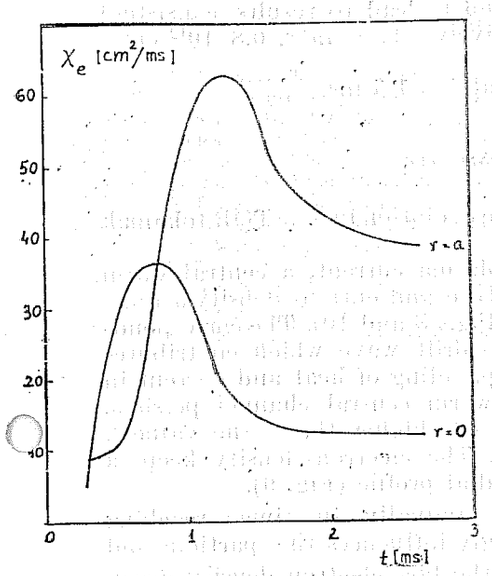

Fig. 7. — The values determined for the thermal conductibility in the centre of the plasma and at its border.

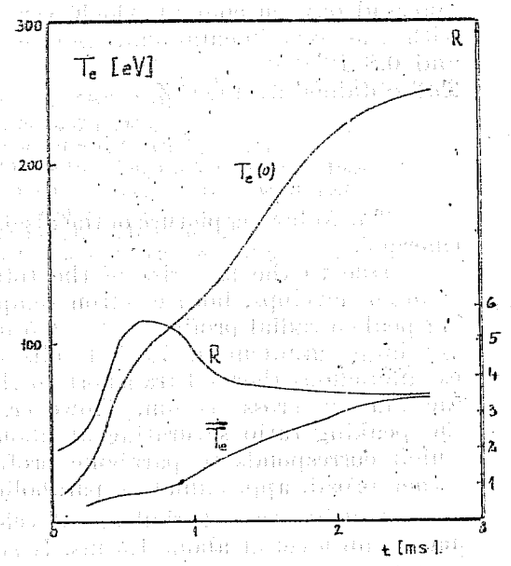

Fig. 8. — The electron temperature determined for the CASTOR discharge : central and average values and the peaking ratio $R = T_e(0)/\bar{T}_e$.

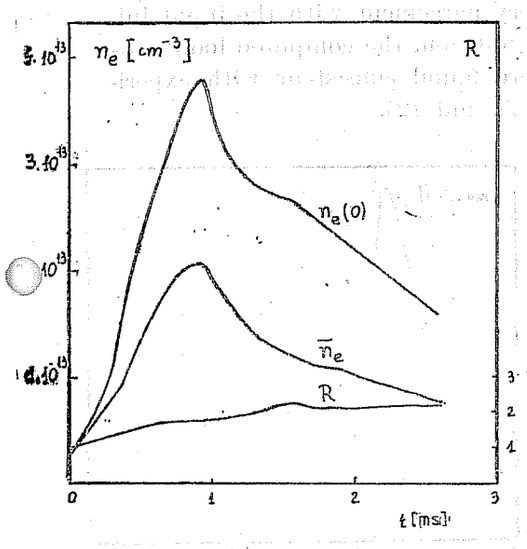

Fig. 9. — The electron density for the CASTOR discharge : central and average values and the peaking ratio $R = n_e(0)/\bar{n}_e$.

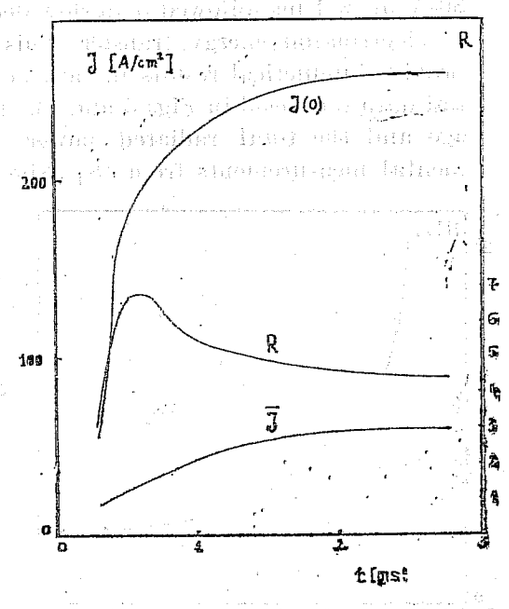

Fig. 10. — The current density determined for the CASTOR discharge : central and average values and the peaking ratio $R = J(0)/\bar{J}$.

bon and oxygen content which were found to lead to results consistent with the experimental data are respectively: 10^{13} cm^{-3}, 0.8 10^{12} cm^{-3} and 0.8 10^{12} cm^{-3}.
The obtained average Z_{eff} was about 3 at $t = 1.5$ ms.

4. CONCLUSIONS

The following picture of the discharge evolution in CASTOR tokamak emerged.

Due to the fast rise of the total plasma current, a central warm channel develops, both electron temperature and current density acquiring peaked radial profiles at $t = 0.5$ ms (Fig.s 8 and 10). The corresponding large gradient of T_e destabilises the drift wave which contributes by anomalous thermal transport to the spreading of heat and current in the plasma cross section. However, a warm central channel persists, the peaking ratio saturating at about 3—4 (higher than the value 2 which corresponds to parabolic profiles). The electron density keeps a rather broad, approximately parabolic radial profile (Fig. 9).

A drift wave turbulence develops gradually in time, reaching maximum level at about 1.5 ms. It strongly influences the particle and heat losses providing the explanation of the fast electron density decay ($t > 1$ ms). The central electron temperature saturates at $\approx$ 250eV (Fig. 8) while the ion component remains cold. It reaches a maximum of about 30eV at $\approx$ 1 ms followed by a slow decay due to the continuous lowering of electron-ion energy transfer. This model of the CASTOR discharge provides numerical results in satisfactory agreement with the input initial data (curves 3 in Figs 3 and 6). In addition, the computed loop voltage and the total radiated power were found consistent with experimental measurements from [8] (Figs. 11 and 12).

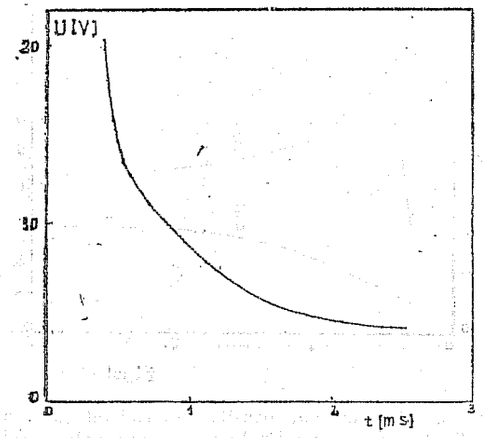

Fig. 11. — The computed loop voltage.

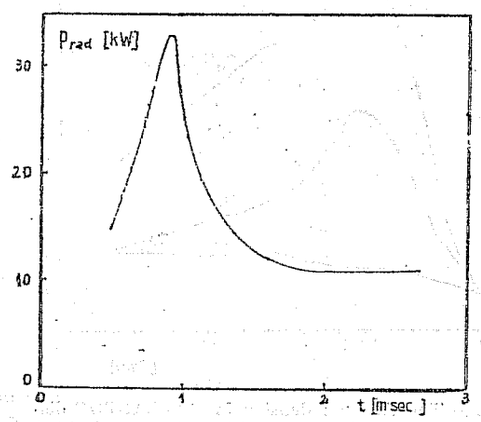

Fig. 12. — The computed radiated power.

REFERENCES

1. Yu N. Dnestrovski, S. V. Neudachin, G. V. Pereverzev, Fizika Plasmy, **10**, 236 (1984).
2. P. H Rutherford, D. F Duchs, Reports MATT—1272 (1976).
3. F. Spineanu, M. Vlad, Rev. Roum., Phys., **30**, 497 (1985).
4. F. Spineanu, M. Vlad, I. I. Popescu, Raport ICEFIZ LOP—47—1984.
5. F. Spineanu, M. Vlad, I. I. Popescu, Comp. Phys. Communications, **41**, 155 (1986).
6. F. Spineanu, M. Vlad, Proceedings of the VIIIth ESCAMPIG, Greifswald, 1986.
7. R. D. Bengston, Diagnostic for Fusion Experiments.
8. K. S. Dyabilin, J. Badalec, A. A. Borschegovski, J. Datlov, K. Jakubka, V. Kopecky, A. A. Korotkov, J. Stockel, M. Valovic, F. Zacek, Czech. Journal of Phys., **B37**, 713 (1987).
9. P. Liewer, Nucl. Fusion, **25**, 543 (1985).
10. W. M. Tang, Nucl. Fusion, **18**, 1089 (1978).
11. V. A Rojanski, Pis'ma Zh. Exp. Teor. Fiz., **34**, 60(1981).